Coastal Engineering 63 (2012) 3–12

Contents lists available at SciVerse ScienceDirect

Coastal Engineering

journal homepage: www.elsevier.com/locate/coastaleng

Barrier dynamics experiment (BARDEX): Aims, design and procedures

J.J. Williams [a,*], D. Buscombe [b], G. Masselink [b], I.L. Turner [c], C. Swinkels [d]

[a] ABPmer, Suite B, Town Quay, Southampton SO14 2AQ, UK
[b] School of Marine Science and Engineering, University of Plymouth, Plymouth, PL4 8AA, UK
[c] Water Research Laboratory, School of Civil and Environmental Engineering, University of New South Wales Sydney, NSW 2052, Australia
[d] Deltares, Rotterdamseweg 185, 2629 HD Delft, Postbus 177, 2600 MH Delft, The Netherlands

ARTICLE INFO

Article history:
Received 21 November 2011
Accepted 9 December 2011
Available online 23 January 2012

Keywords:
Gravel barrier
Delta flume
Waves
Tides
Prototype scale experiment

ABSTRACT

Although relatively common features in nature, only a handful of laboratory studies have examined the dynamic response of gravel beaches and barriers to combined tidal and wave forcing and to storm simulations. This paper reports experiments undertaken in the Delta flume during the BARDEX project using a prototype gravel barrier (55 m-long, 5 m-wide and 4 m-high with seaward and lagoon facing slopes of 1 V/8H and 1 V/4H, respectively) composed of sub-rounded gravel (D_{50} = 11 mm). Hydrodynamic conditions and beach morphology were measured using buried PTs, ECMs and closely spaced bed location sensors on a scaffold frame spanning the entire barrier. Additional measurements were also obtained from video and from instruments on an offshore frame. A series of systematic tests were undertaken using pumps to change water levels on the seaward (h_S) and lagoon (h_L) sides of the barrier. These included: 1) hydraulic conductivity tests where h_S and h_L levels were varied; 2) tests to assess the impact of waves (h_S = 2.5 m, variable h_L in the range 1 m to 2.5 m, significant wave height, H_s = 0.8 m, and peak wave period, T_p = 3.0 s, 4.5 s and 6 s); 3) tests examining the effect of tides (varying h_S from 1.75 m to 3.25 m, variable h_L at high ($h_L = h_S + 1$ m), medium ($h_L = h_S$) and low ($h_L = h_S - 1$ m) levels, H_s = 0.8 m and T_p = 4.5 s); and 4) overwash tests (tidal simulation, variable h_L, H_s = 1 m and T_p = 4.5 s, 6 s, 7 s and 8 s). The principal objective of the paper is to provide essential information on the design and execution of the BARDEX experiments referred to in the series of papers that follow in this special edition. It also describes the instrumentation used to measure hydrodynamic, morphodynamic and sediment processes.

1. Introduction

The BARDEX experiments were motivated by two main considerations. (1) Gravel beaches provide effective natural sea defences from flooding at many worldwide locations (e.g. Bradbury and Powell, 1992; Mason and Coates, 2001; Obhrai et al., 2008; Pedrozo-Acuna et al., 2007) and many are currently actively eroding (e.g. Chadwick et al., 2005; Pye and Blott, 2009). This process increases the threat to coastal infrastructure, exacerbates coastal flooding problems and may possibly lead to further loss of important natural habitats. The processes responsible for the formation, maintenance and erosion of gravel beaches and barriers are not fully-understood and require further work (e.g. Masselink and Buscombe, 2008). (2) Coarse sediment is increasingly used for beach nourishment and recharge in coastal protection schemes (e.g. Lawrence et al., 2002; Moses and Williams, 2008; Riddell and Young, 1992; Van Wellen et al., 2000) and attracts an annual expenditure of c. 60 million Euros in the UK alone (Bradbury and McCabe, 2003). The further development, testing and validation of numerical models to assist with scheme design and to assess the response of gravel coastlines to a range of storm and sea level scenarios is thus desirable from a coastal engineering and management perspective (e.g. Bradbury, 2000).

Most of the world's gravel beaches are found in meso- to macrotidal settings, and thus tidal effects on beach morphodynamics cannot be ignored (Masselink and Short, 1993). Furthermore, owing to the coarse nature of the sediments, beach porosity can also exert a significant influence on morphodynamic behaviour. However, most previous laboratory flume experiments have used a fixed mean water level to study the response of gravel beaches to waves (e.g. Roelvink and Reniers, 1995). Although a few studies have attempted to examine the response of gravel beaches to waves and tides (e.g. Trim et al., 2002), the experiments are subject to scaling problems and the beaches used are normally emplaced on impermeable ramps at the end of the test facilities. Such experiments fail, therefore, to replicate some important aspects of natural gravel beach hydrology. Moreover, many gravel beaches (with a hydraulic conductivity greatly exceeding that of sand beaches) are barrier beaches which front and protect low-lying coastal areas (lagoons, estuaries, and coastal plains) from coastal flooding. Examples in the UK include Westward Ho!, Porlock,

* Corresponding author. Tel.: +44 23 80711840; fax: +44 23 8071 1841.
E-mail addresses: jwilliams@abpmer.co.uk (J.J. Williams), g.masselink@plymouth.ac.uk (G. Masselink), ian.turner@unsw.edu.au (I.L. Turner), Cilia.Swinkels@deltares.nl (C. Swinkels).

0378-3839/$ – see front matter © 2011 Elsevier B.V. All rights reserved.
doi:10.1016/j.coastaleng.2011.12.009

Slapton Sands, Chesil and Blakeney. Being subjected to relative changes in water level on both their seaward and landward sides, hydraulic gradients are likely to be an important element governing their dynamics and stability.

In order to replicate as many of the natural processes as possible in the BARDEX experiments, a prototype scale open-coast tidal beach composed entirely of medium gravel was emplaced in the Delta flume in the Netherlands and subjected to simulated tidal modulations and to waves. The primary objective was to obtain data required to understand, parameterise, model and predict gravel beach morphodynamics. For that purpose experiments were undertaken using a range of water levels on either side of the barrier, with time-varying water level on the seaward side of the beach being used to simulate tides. Detailed measurements were taken of: 1) the nearshore flow field and sub-tidal bedforms; 2) swash hydrodynamics; 3) beach/bed-levels and 4) the beach water table. In order to address the problem of parameterising and modelling the incipient conditions for natural overwashing and barrier failure during storms, another set of experiments simulated tidal modulation and wave conditions typical of storms. In such conditions, gravel barrier overwashing can sometimes lead to breaching and contribute, over time, to large-scale roll-back (Forbes et al., 1991). This process has implications for long-term coastal managements and is therefore one requiring investigation.

Owing to an abundance of sediments with a median diameter, D_{50}, >2 mm, gravel beaches and barriers are common along formerly (peri-) glaciated coasts. In some cases these sediments may be derived from erosion of terrestrial glacial deposits (e.g. Orford et al., 1996) or from the continental shelf during the Holocene transgression (e.g. Long et al., 2006; Plater et al., 2009). At other locations coarse beach material may be supplied from fluvial sources (e.g. Shulmeister and Kirk, 1997) or through cliff erosion (e.g. Pye and Blott, 2009). As a general rule, gravel beaches are mostly frequently encountered in wave-dominated coastlines at mid- and high latitudes with meso- or macro-tidal regimes.

Studies examining the long-term evolution of gravel barriers in response to changes in relative sea level, and to variations in the sediment supply (*cf.* Orford et al., 2002), have highlighted the importance of overwashing (Orford et al., 1988), or even breaching, during extreme storm conditions (Orford et al., 2003). On shorter time-scales studies of the dynamics of the beach step and the evolution of the berm over consecutive tides (e.g. Austin and Buscombe, 2008) have identified the importance of swash processes and the important role of swash-groundwater interactions in the development of gravel beach morphology (e.g. Austin and Masselink, 2006a). Specifically, because gravels are significantly more porous than beach sands, they exert important control on a number of key beach processes. For example, studies of interactions between swash flows and the beach groundwater have demonstrated a significant effect on beach morphology and stability attributable to swash infiltration into the (upper) unsaturated beach; and infiltration and exfiltration across the (lower) saturated beach (e.g. Butt et al., 2001; Horn, 2006; Puleo, 2009; Turner and Masselink, 1998; Masselink and Turner (this volume)). Although some aspects of gravel beach hydrodynamics can be inferred from measurements of the beach profile and from the sediment grain size distribution and changes in sorting (e.g. Austin and Masselink, 2006b), the measurement in the field of hydrodynamic parameters required in existing models (e.g. Bradbury and Powell, 1992; Pedrozo-Acuna et al., 2006; 2007), or in predictive statistical approaches (e.g. Kroon et al., 2008) is extremely difficult owing to the very energetic nature of the breaker zone. Thus providing some scaling issues can be resolved, there is therefore a great deal that can be learned about processes and about hydrodynamic processes and the morphodynamic responses from a series of controlled large-scale experiments in which a gravel barrier is subjected both to simulated tidal motion and a range of wave conditions.

The BARDEX project has four objectives and all experiments were designed to provide high-quality data sets for process studies and for numerical model calibration and testing: 1) to investigate the role of back-barrier lagoon levels on the dynamic groundwater profile through the barrier and to assess whether varying groundwater levels may induce different morphological response at the beach face; 2) to improve the understanding of sediment transport processes on the beach face under conditions of accretion and erosion; 3) to examine hydrodynamics and sediment transport at locations from the swash region to locations offshore from the barrier; and 4) to improve the understanding of overwash sediment transport and the threshold conditions for overwash occurrence. The data acquired have been used to examine the prognostic capabilities of the XBeach numerical model (Williams et al., this volume).

2. Methods

2.1. Construction of the gravel barrier and water level control

The scale of the Delta flume (240 m-long, 5 m-wide, 7 m-deep) enabled the experiments to be conducted with natural gravel, which avoids the adverse scale effects. Using locally sourced fluvial gravel with a median grain size, D_{50}, ~11 mm, a 55 m-long, 4 m-high and 5 m-wide gravel barrier crest was constructed in the central region of the Delta flume. The barrier was carefully profiled to give a gradient of 1 V/8H for the slope facing the wave paddle and a 1 V/4H gradient for the opposite slope (Fig. 1). Fig. 2 shows the physical characteristic of the barrier sediments. The mid-barrier crest was located at an along flume distance, X, from the wave paddle of approximately 95 m (Fig. 1) and the flume volume between the barrier and the wave paddle (hereafter called 'sea') was filled with water to a required depth. In addition, owing to a unique feature of the Delta flume, it was possible to create a 'lagoon' between the back slope of the barrier and a watertight gate emplaced at $X\sim130$ m (Fig. 1). As complete barrier overwash tests were planned, a series of effective wave absorption baffles were constructed behind the barrier at the end of the lagoon to reduce wave reflection (Fig. 1). The water levels in the sea and lagoon were maintained at set levels by 4×180 l/s pumps with connecting pipe work and a flow control system (Fig. 1). The flume channel behind the gate was filled with water and acted as a reservoir to supply water to, and to store water from, the sea and lagoon. The pumping system was able to maintain the water levels either side of the barrier to a tolerance of ±10 mm, permitting the simulation of differing sea-level, tidal and beach groundwater conditions. Pump discharges in and out of the lagoon were measured using a Siemens *Magflow 5100* and enabled direct determination of flow rates through the barrier when a hydraulic gradient was applied. The effects on beach profile development attributable to a range of wave and water level conditions (tides) were investigated by raising and lowering the water level on the seaward side of the barrier and in the lagoon.

2.2. Water levels and wave generation

In most BARDEX tests the sea and lagoon water depths were maintained at the required levels by the pumping system. Test waves were then generated using a JONSWAP wave steering signal specified by significant wave height, H_s, and peak wave period, T_p using default settings for gamma (3.3) and sigma (0.07 and 0.09 for sigma low and sigma high respectively). This latter parameter represents the narrowness of the spectrum. Wave groupiness, caused by constructive or destructive interference is a function of the spectral form and was not user defined (*cf.* Battjes and van Vledder, 1984). In most tests, reflected waves, as well as low-frequency resonant waves were damped at the paddle using an Automated Reflection Compensator (ARC). In Fig. 3a the power spectral density (PSD)

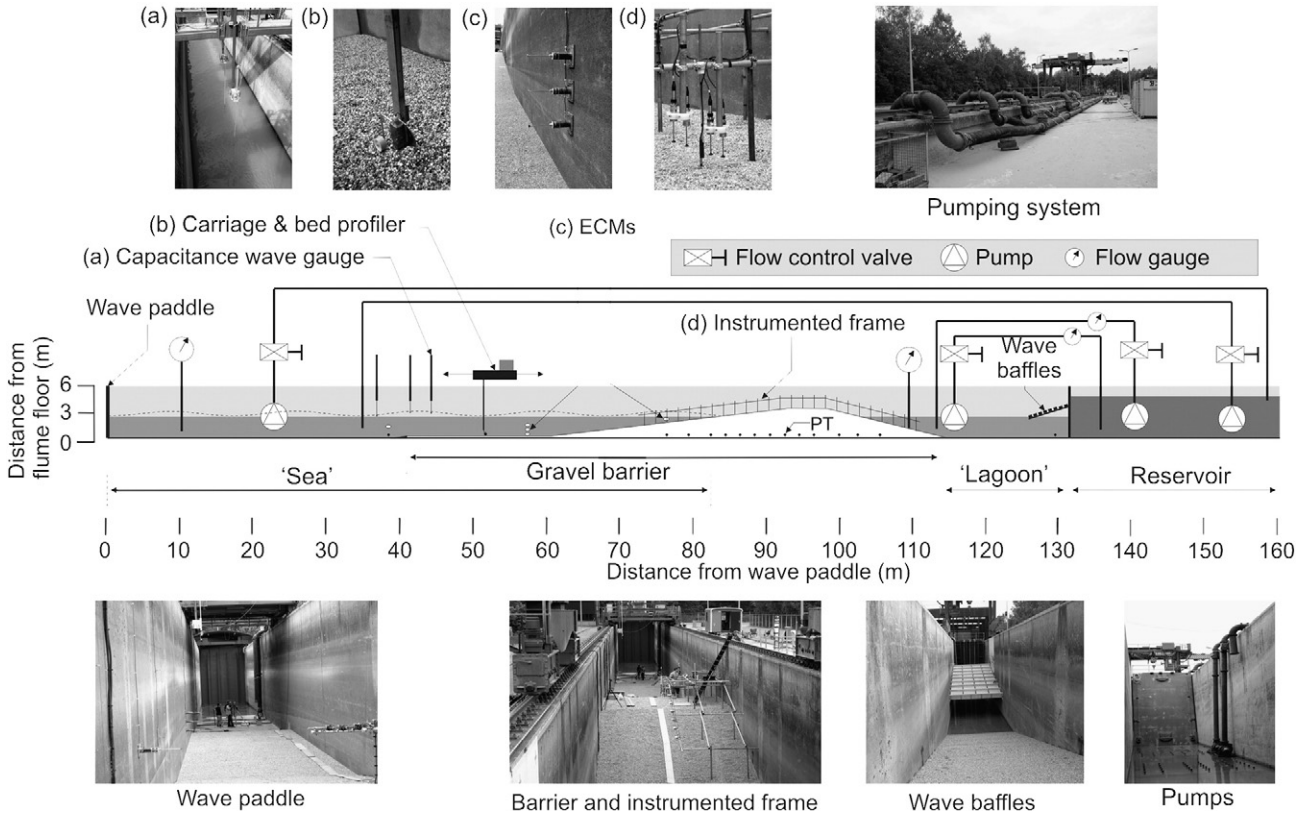

Fig. 1. Diagram of the BARDEX experiment showing the location of the gravel barrier in the Delta flume in relation to the wave paddle and the reservoir section. The pumping system is shown schematically and photographs are used to illustrate key features of the Delta flume and associated instrumentation.

functions are shown for waves measured by a pressure sensor in tests *C5-4*, *C1-4* and *B2-4* and in Fig. 3b water surface elevation measured by the WG at $X = 41$ m during test *E8-6*. This wave sequence was repeated throughout all series *E* tests and included a single large *overwash initiation* wave at approximately 135 s from the start of the sequence. This was intended to overtop the barrier to remove any residual berm from the proceeding test and to promote subsequent overwashing by smaller waves in the sequence. In the event this was successful. H_s and T_p values were obtained by spectral analysis of PT data (*cf.* Bishop and Donelan, 1987). In all cases there was close agreement between design and test conditions in the BARDEX test. Further details of wave generation and properties are given by Buscombe et al. (2008).

2.3. Sediment properties

Five 25 cm long cores of sediment were collected at locations across the top of the barrier profile by pushing 5 cm-diameter Perspex tubes into the gravel and sealing the ends *in situ*. This was designed to yield some information on the potential sorting of the gravel near the surface of the barrier. The tests were carried out before any overwash experiments took place and sorting was minimal. The grain size distribution was obtained by sieving for the gravel material as it was delivered to the flume (Fig. 2a). The material is a moderately well sorted, unimodal medium gravel (Fig. 2b) with a median grain size (D_{50}) of 11.0 mm ($D_{10} = 5.4$ mm, $D_{90} = 16.9$ mm). The distribution is fine skewed and leptokurtic as defined by the Folk and Ward (1957). The particle shape distribution for a random sample of barrier sediments is shown in Fig. 2c. Routine measurements of mean grain size for surficial sediments were obtained at various stream-wise locations across the barrier between each experiment using the photograph techniques based on Rubin (2004) described by Buscombe and Masselink (2009). The grain size distributions were also determined using the same images following the method of Buscombe (2008). Larger samples obtained using similar techniques were used to determine the sediment porosity,*n*, defined volume of voids / volume of voids plus gravel. The average value for *n* was found to be 0.32 with a standard deviation of 0.04. The sediment density was also determined from a bulk sample and found to be 2630 kg/m^3.

2.4. Hydrodynamic measurements

The incident wave field, and associated wave induced flows were measured offshore using three wave gauges (WGs) and five 40 mm-diameter Marsh-McBirney 511 electromagnetic current meters (ECMs) mounted on the side wall of the flume (Fig. 1). The WGs comprised a vertical aluminium gauge with a conductivity sensor at the bottom tip. A servo motor moved the gauge vertically so that the tip remained just in contact with the water surface. These wave height data, in combination with measurements of the horizontal and vertical flow components from a single ECM, were sufficient to describe the incoming and outgoing wave characteristics (spectra) accurately. The distances between the wave followers were periodically adjusted, depending on the steepness of the waves, as prescribed by Mansard and Funk (1980) in their method for derivation the incident spectrum from the measured water surface elevation. In order to measure the pressure profile, and to thereby infer the phreatic surface, the barrier was instrumented with *Druck PTX 1830* pressure transducers, PTs, (1 bar range; absolute accuracy of 0.4%, Fig. 1). These were deployed 0.035 m above the floor of the flume at $X = 38$ m and from 76 m$< X <$106 m with a normally at a spacing of 2 m to 3 m. Table 1 summarises the streamwise (X), spanwise (Y) and vertical (Z) locations of these instruments where $X, Y, Z = 0$ is located at the wave paddle on the floor of the flume next to the left wall. It also gives the measurement units of each sensor.

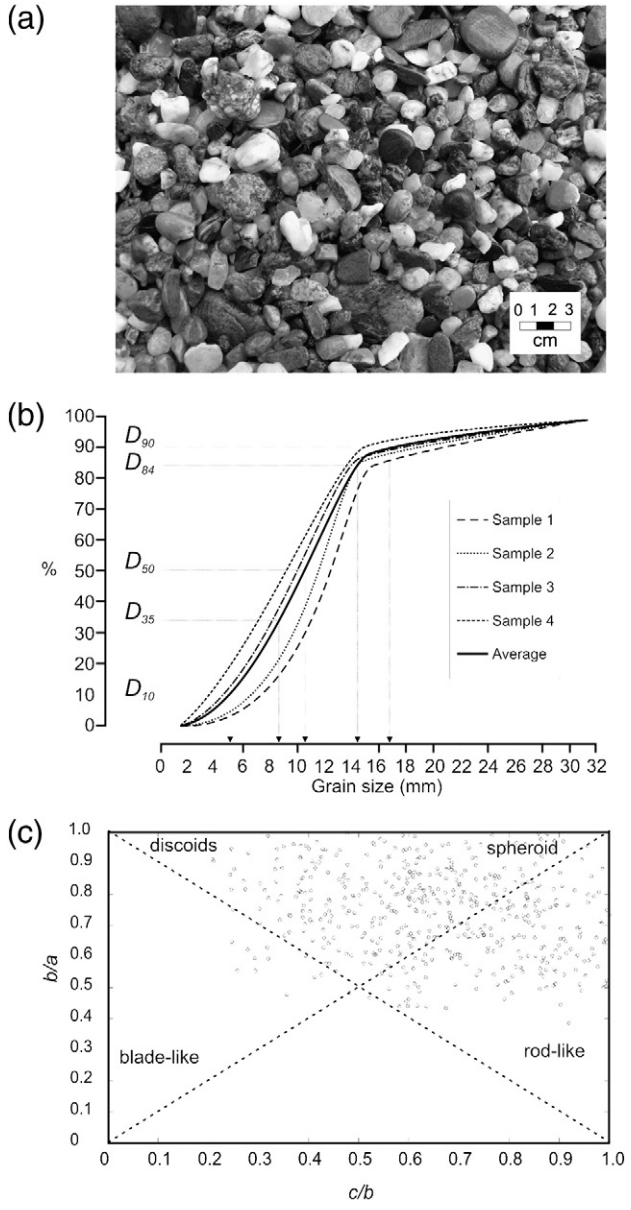

Fig. 2. (a) Close-up of barrier sediments. (b) Barrier sediments grain size distribution obtained by sieving of BARDEX sediments. (c) Particle shape distribution for a random sample of barrier sediments.

A scaffold support frame (30 m-long and 2 m-wide) spanning the barrier from 76 m<X<110 m was used to support four mini (*Valeport* with disc-shaped head) at X = 82.5 m, (Fig. 1). Although these were deployed at various elevations from the bed to record swash velocities, there was always one ECM deployed at *c.* 0.03 m from the bed to record the near-bed flow velocity. The same ECM elevations relative to the evolving barrier profile were maintained throughout the tests by manual adjustment during periods of no waves. Additional ECM pairs were also deployed from the frame at locations further up the beach determined by wave conditions during any given test. Following adjustments, all instrument positions were surveyed using a *Trimble 5605* Robotic Total Station to a local coordinate system. A similar frame construction has been used successfully to deploy instruments in field experiment at Truc Vert, France, and at Slapton Sands, UK (e.g. Masselink et al., 2009).

A vertical array of three absolute PTs (*Druck PDCR1830*) were co-located with the ECMs on the frame and buried in the bed at 0.1 m, 0.25 m and 0.4 m depth to record vertical pressure gradients at X = 82.5 m. Additional absolute PTs (*Druck PDCR1830*) were installed at *c.* 0.03 m from the bed surface to record the swash depth at each of the ECM stations to help identify the times when the ECM closest to the bed was submerged. The location of these instruments was adjusted between each test as required to maintain the required burial depth. An absolute PT (*Druck PDCR1830*) was also deployed to record the atmospheric pressure, required to convert the absolute pressures recorded by the PTs to hydrostatic pressure and water depth. Data from these instruments, related to swash flow velocities and depths, were recorded at 4 Hz. To record wave run-up, a *Sony SSC-DC50AP* video camera positioned on the profiling gantry high above the centre of the flume, and facing the waves, was used. Images were referenced to ground control point positions and recorded at 4 Hz into Matlab data files following image orthorectification. These images were subsequently digitally filtered to remove strong gradients in sunlight across the flume.

A frame was used to deploy instruments at locations seaward of the barrier to measure wave-induced turbulence and bed morphology (Fig. 4). These comprised a *Sontek* 10 MHz autonomous *Hydra ADV Ocean Probe* with strain-gauge pressure and water temperature sensors and compass and inclinometers recording at 25 Hz and two cabled *Nortek* 10 MHz *Vectrino* ADVs recording at 25 Hz. These instruments were used to measure wave-induced turbulence at nominal heights z above the bed of 0.06 m, 0.25 m and 0.5 m. In addition, two autonomous *Marine Electronics* acoustic bed profilers (ABP) were deployed on the frame to measure the bed morphology. The ABPs operated at 2 MHz with a 1.1° conical beam and were mounted horizontally on the frame to scan a cross-section of the bed over an angular range of 120°. The frame was deployed at locations seaward of the wave breaking zone using the Delta flume gantry crane (Fig. 4) and was carefully aligned with the side wall of the flume using projecting guides fixed to the frame.

2.5. Morphodynamic measurements

Barrier profiles were measured at the end of each wave sequence using a roller and actuator which followed the bed profile from an overhead carriage, thereby allowing supra-tidal and sub-tidal profiles to be measured with identical accuracy (Fig. 1). An array of 45 temperature compensated *Massa M300/95* ultrasonic proximity sensors operating at 95KHz, and recording data at 4 Hz were deployed at *c.* 1 m from the bed at 0.5 m intervals on the scaffold frame (Figs. 1 and 5). Each had a beam angle of 8° giving a measurement footprint c. 28 cm in diameter and a vertical accuracy of *c.* ±1 mm. Data for temperature corrections were supplied from a locally installed meteorological station mounted above the flume. In addition to providing direct measurements of bed level between swash events, these data were also used to derive flow depths and velocities associated with individual swash and backwash events (Turner et al., 2008).

2.6. Sediment tracers

Sediment tracers were used in *Test Series E6* to assess obliquity of overwash sediment transport across the back-barrier. Using a fluorescent paint three 30 kg samples of barrier gravel were dyed using three colours (orange, green and blue). The application of the dye to the surface had no measureable effect on the physical or hydrodynamic properties of the sediment. Before overwash tests, sediment tracers were placed flush with the barrier surface at three locations along the crest. Samples of surficial sediments were obtained after periods of overwash and analysed using a UV light source to determine the transport pathways. No significant transverse gradients in transport were detected.

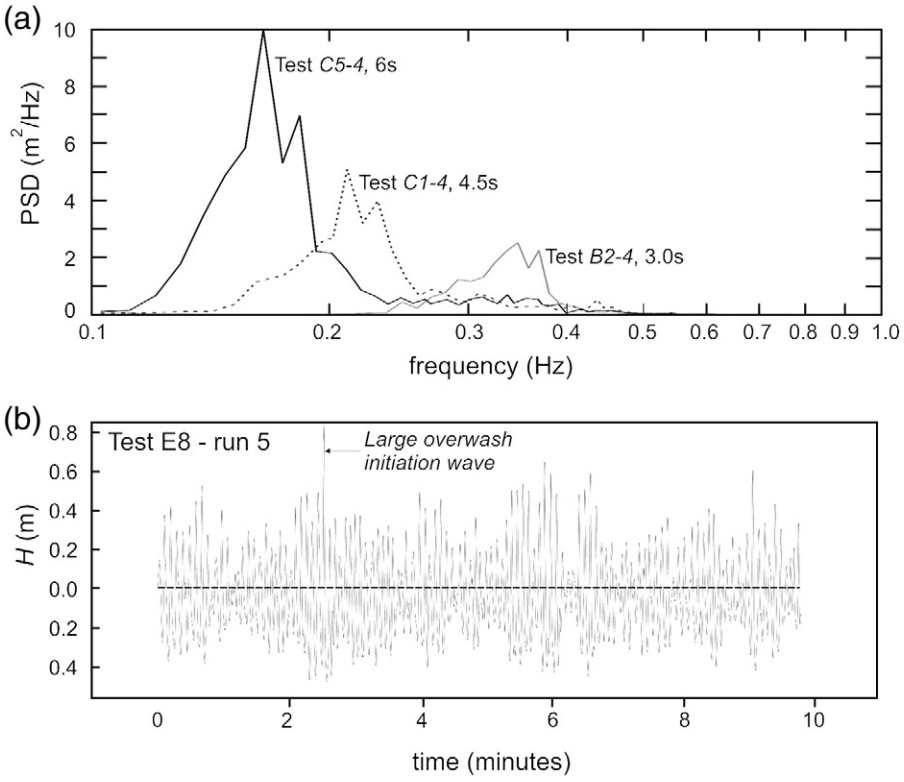

Fig. 3. (a) Power spectral density (PSD) functions for waves measured by a PT at $X = 76$ m in tests *C5-4*, *C1-4* and *B2-4*. (b) Water surface elevation measured by a WG at $X = 41$ m during test *E8-6* showing the single large *overwash initiation* wave.

3. Data logging, processing and storage

With the exception of the autonomous instruments on the offshore frame, all other instruments were linked to a number of

Table 1
Summary of wave gauge, pressure sensor and electromagnetic current meter locations during the BARDEX experiments.

Sensor	*X*	*Y*	*Z*	units
WG01	36.7	0.5	3.500	m
WG02	41.0	0.5	3.500	m
WG03	43.9	0.5	3.500	m
Druck PTX 1830	76.0	0.25	0.035	kN/m^2
Druck PTX 1830	79.0	0.25	0.025	kN/m^2
Druck PTX 1830	82.0	0.25	0.035	kN/m^2
Druck PTX 1830	84.0	0.25	0.035	kN/m^2
Druck PTX 1830	86.0	0.25	0.035	kN/m^2
Druck PTX 1830	88.0	0.25	0.035	kN/m^2
Druck PTX 1830	90.0	0.25	0.035	kN/m^2
Druck PTX 1830	92.0	0.25	0.035	kN/m^2
Druck PTX 1830	94.0	0.25	0.035	kN/m^2
Druck PTX 1830	96.0	0.25	0.035	kN/m^2
Druck PTX 1830	99.0	0.25	0.035	kN/m^2
Druck PTX 1830	102.0	0.25	0.035	kN/m^2
Druck PTX 1830	105.0	0.25	0.035	kN/m^2
Druck PTX 1830	38.3	0.25	0.035	kN/m^2
Druck PTX 1830	129.0	0.25	0.035	kN/m^2
Druck PTX 1830	140.0	0.25	0.035	kN/m^2
Marsh-McBirney 511 ECM	57.0	0.59	1.350	m/s
Marsh-McBirney 511 ECM	57.0	0.59	1.350	m/s
Marsh-McBirney 511 ECM	57.0	0.59	1.750	m/s
Marsh-McBirney 511 ECM	57.0	0.59	1.750	m/s
Marsh-McBirney 511 ECM	57.0	0.59	2.150	m/s
Marsh-McBirney 511 ECM	57.0	0.59	2.150	m/s
Marsh-McBirney 511 ECM	76.0	0.59	2.100	m/s
Marsh-McBirney 511 ECM	76.0	0.59	2.100	m/s
Marsh-McBirney 511 ECM	38.4	0.59	1.000	m/s
Marsh-McBirney 511 ECM	38.4	0.59	1.000	m/s

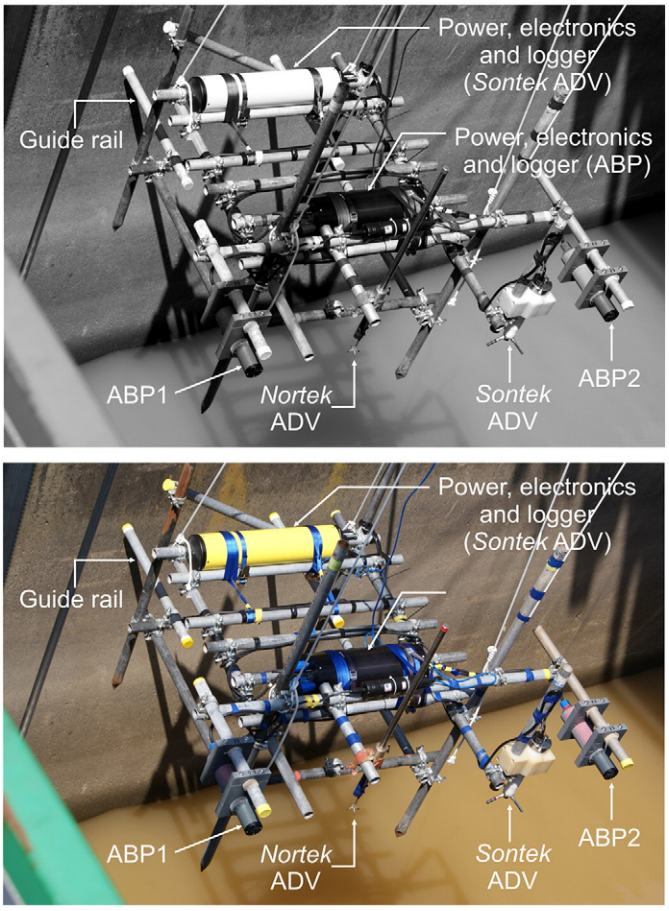

Fig. 4. The offshore frame with ABPs and ADVs and associated power supplies and data logging units. The photograph shows deployment before test B3.

Fig. 5. Photograph looking toward the wave paddle showing part of the array of ultrasonic bed level sensors on the scaffold frame and the swash ECMs and PT.

networked laptop and desktop PCs to record data. All logging computers were synchronised from a GARMIN GPS using TAC32 software. Similarly, the autonomous logging systems were also synchronised to this common time-base. Further details are given by Buscombe et al. (2008). Depending on the test run, the number of logged data channels varied from 87 to 119. To provide a convenient way to group related data of different types all raw data were organised into 28 data structures for each experiment. Data fields were ascribed for each related group of measurements (e.g. PT and ECM data) and sub-fields were used to hold individual data sets. 1.5 GB of quality-controlled data were stored on a single DVD which also included some Matlab scripts to load data and perform some elementary analysis. These data can be read by Matlab or Octave. This proved to be an effective way for the BARDEX scientists to access the data and to make the data available to other interested groups.

4. BARDEX experiments

4.1. Test series

The initial Test Series A was performed in the absence of waves for the purpose of assessing barrier stability when subjected to a range of hydraulic gradients induced by varying sea/lagoon water levels, and to test and fine-tune the pump the controller system used for all subsequent tests to maintain the required sea and lagoon water levels. The four tests series followed were then undertaken to examine barrier profile response to: 1) waves only (*Test Series B*); 2) waves with a fixed offshore water level and varying lagoon levels (*Test Series C*); 3) waves and simulated tidal cycles (*Test Series D*); and 5) storm conditions using tidal simulation and large waves (*Test Series E*). Fig. 6a shows sea, h_S, and lagoon, h_L, water levels set during all the BARDEX tests. It shows tests with fixed h_S levels and tests involving tidal simulations. The corresponding H_s and T_p values for all BARDEX tests are shown in Fig. 6b.

4.2. Design of the test sequence

Since *Test Series C* and *D* aimed to examine if the beach groundwater profile affected barrier morphodynamics in different wave conditions, it was necessary to simulate the same sea level, tidal modulation, wave forcing and antecedent morphology in every test and only vary the barrier water table. Although accurate replication of sea level, tidal signal and wave forcing was possible, the large size of the barrier made re-profiling between tests impracticable and thus a test chronology was designed to reduce the dependency on initial conditions of subsequent barrier profile developments. The resulting chronological sequence of tests undertaken in BARDEX are summarised in Table 2. This table gives h_S, h_L, H_s and T_p values, the duration of a test and status of the ARC, and comments relating to the nature of the waves and tide during a given test. This test sequence in Table 2 was intended to ensure that the initial barrier profiles of a given test pair with different lagoon levels (e.g. *C1*/*C2*, *C3*/*C4*, *C5*/*C6* and *D2*/*D3*) were similar. Masselink and Turner (this volume) demonstrate that this was achieved reasonably well, indicating strongly that the main difference between the tests using differing lagoon levels was related to changes in the beach water table and not to the starting morphology of the barrier.

4.3. Test Series B and C

The following illustrates the main features of the test procedure undertaken during *Test Series B and C*. It is subdivided into 5 steps lasting *c.* 8 hours in total. 1) The water level on either side of the barrier was adjusted to the required level and the zero offsets of the buried PTs were adjusted to the ambient atmospheric pressure. 2) To ensure that starting profiles for tests with the same wave conditions, but different lagoon levels, were comparable, the h_S was raised to 2.5 m for a given test, and the barrier was exposed to monochromatic waves (Table 2) with design height, H, and period, T, for 60 min. Although in most tests H and T were set to the H_s and T_p values of the following test, early trials used $H = 1$ m and $T = 10$s for a period of 3 min (Table 2). This approach was abandoned in favour of the former owing to undesirable erosion of the barrier. The heights of the instruments on the scaffold frame were then adjusted and the starting barrier profile was surveyed. 3) The level of the lagoon was then adjusted to the required level for the test and pumps were run continuously to maintain the water levels on each side of the barrier, allowing time for the water table to equilibrate. 4) The test series was then initiated using a 90-min long wave signal divided into nine segments of unequal length (4×5 min; 2×10 min; 2×15 min; and 1×20 min) to enable interruption of the wave action for beach surveys and equipment maintenance. Importantly, for tests with the same wave forcing (H_s and T_p), the identical segmented wave steering signal was used. To enable ensemble averages of the swash/hydrodynamic parameters to be calculated, monochromatic 'reset' waves were again used at the end of the final 'run' for a period of 5 min. 5) After completion of the test, the pumps were stopped and the water levels were allowed to equilibrate, normally overnight.

It was found to be difficult to maintain a constant h_S value using the automated pump system, whilst at the same time suppressing reflection at the paddle using the ARC. Further, without the ARC on, it was difficult to keep the h_S steady. It was found that the best solution was to leave the ARC on and to control the pumps manually. Although requiring some skill, accurate h_S and h_L levels could be maintained using this approach.

4.4. Test Series D and E

It was required in *Test Series D* and *E* to simulate a tidal cycle characterised by a range of sea water levels, h_S, of 1.5 m. Typically, a tidal cycle comprised 14 segments, each lasting 15 min: the first segment

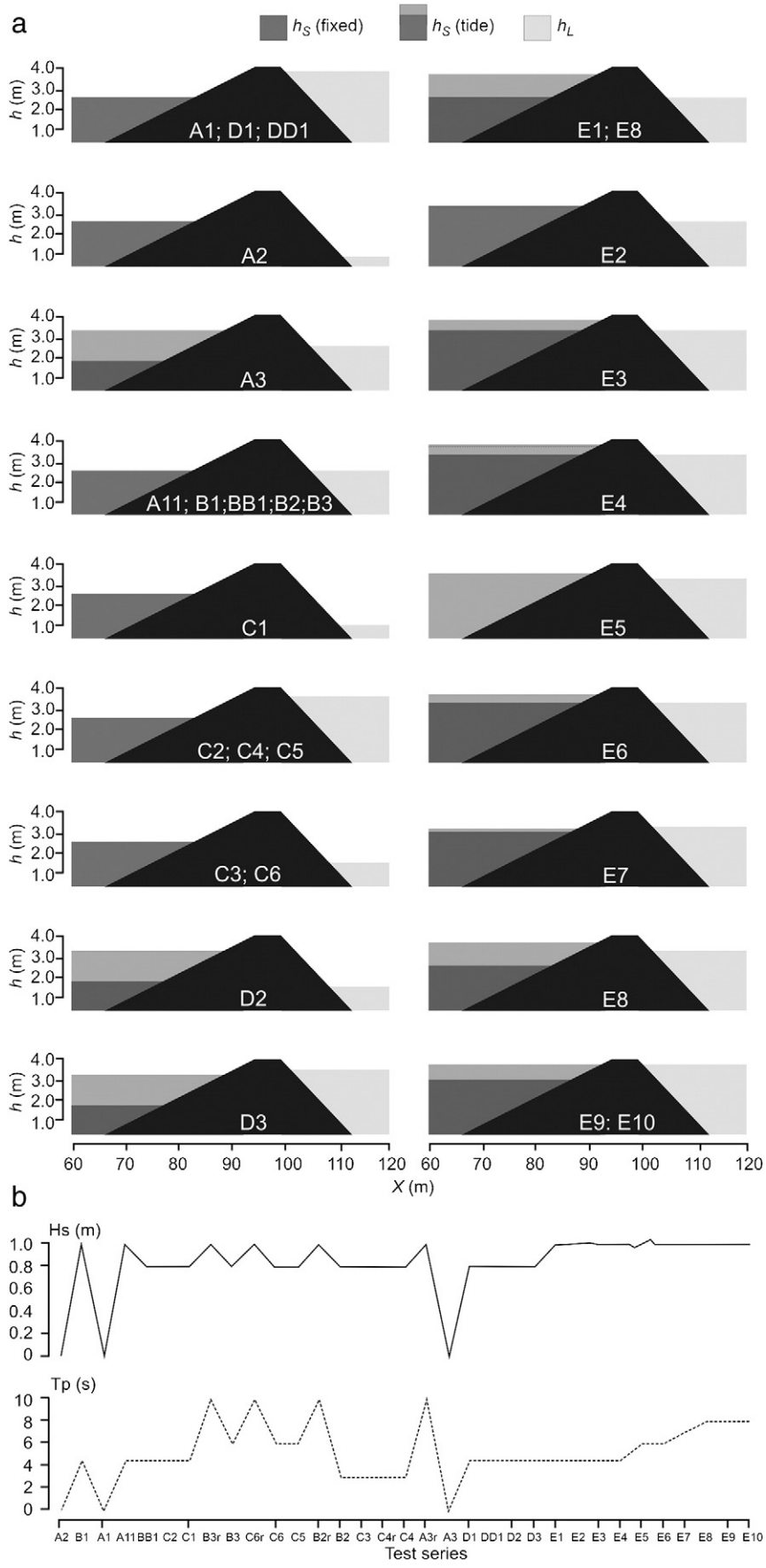

Fig. 6. (a) Schematic summarising planned sea, h_S, and lagoon, h_L, water levels set during all the BARDEX tests. It shows tests with fixed h_S levels and tests involving tidal simulations. (b) H_s and T_p values used for all BARDEX tests.

Table 2
Summary of planned sea and lagoon water level, wave conditions and ARC settings during all BARDEX experiments.

Test	h_S (m)	h_L (m)	*H* or *Hs* (m)	*T* or *Tp* (s)	time (min)	ARC	Comments
A2	2.50	0.80	0.0	0.0	0	n/a	No waves, no tides
B1s	2.50	2.50	1.0	4.5	30	Off	JONSWAP waves, no tide
B1	2.50	2.50	1.0	4.5	55	Off	JONSWAP waves, no tide
A1	2.50	3.80	0.0	0.0	0	n/a	No waves, no tides
A11	2.50	2.50	1.0	4.5	0	n/a	Mono waves, no tide
BB1r	2.50	2.50	0.8	4.5	60	Off	Mono waves, no tides
BB1	2.50	2.50	0.8	4.5	90	Off	JONSWAP waves, no tide
C2	2.50	3.50	0.8	4.5	90	Off	JONSWAP waves, no tide
C1r	2.50	2.50	0.8	4.5	60	Off	Mono waves, no tides
C1	2.50	1.00	0.8	4.5	90	On	JONSWAP waves, no tide
B3r	3.00	2.50	1.0	10.0	3	On	Mono waves, no tides
B3	2.50	2.50	0.8	6.0	90	On	JONSWAP waves, no tide
C6r	2.50	2.50	0.8	6.0	3	On	Mono waves, no tides
C6	2.50	3.50	0.8	6.0	90	On	JONSWAP waves, no tide
C5r	2.50	2.50	0.8	6.0	3	On	Mono waves, no tides
C5	2.50	1.50	0.8	6.0	90	On	JONSWAP waves, no tide
B2r	3.00	2.50	1.0	10.0	3	On	Mono waves, no tides
B2	2.50	2.50	0.8	3.0	90	On	JONSWAP waves, no tide
C3r	2.50	2.50	0.8	3.0	3	On	Mono waves, no tides
C3	2.50	1.50	0.8	3.0	90	On	JONSWAP waves, no tide
C4r	2.50	2.50	0.8	3.0	3	On	Mono waves, no tides
C4	2.50	3.50	0.8	3.0	90	On	JONSWAP waves, no tide
A3r	2.50	2.50	0.0	0.0	0	n/a	No waves, no tides
A3	1.75 to 3.25	2.50	0.0	0.0	0	n/a	No waves, tides
D1r	2.50	2.50	1.0	10.0	3	On	Mono waves, no tides
D1	1.75 to 3.25	2.50	0.8	4.5	75	On	JONSWAP waves, tide
DD1	1.75 to 3.25	2.50	0.8	4.5	90	Off	JONSWAP waves, tide
D2	1.75 to 3.25	1.50	0.8	4.5	90	Off	JONSWAP waves, tide
D3	1.75 to 3.25	3.50	0.8	4.5	90	Off	JONSWAP waves, tide
E1	3.00 to 3.63	2.50	1.0	4.5	90	On	JONSWAP waves, tide
E2	3.25	2.50	1.0 to 1.2	4.5	60	On	Increasing JONSWAP, no tide
E3	3.25 to 3.75	3.25	1.0	4.5	75	On	JONSWAP waves, tide
E4	3.63 to 3.25 to 3.75	3.25	1.0	4.5	120	On	JONSWAP waves, tide
E5	3.50	3.25	0.8 to 1.3	4.5	90	On	Increasing JONSWAP, no tide
E6	3.25 to 3.63	3.25	1.0	6.0	60	On	JONSWAP waves, tide
E7	3.00 to 3.13	3.25	1.0	7.0	30	On	JONSWAP waves, tide
E8	2.50 to 3.63	3.25	1.0	8.0	135	On	JONSWAP waves, tide
E9	3.00 to 3.75	3.25	0.8	8.0	150	On	JONSWAP waves, tide
E10	3.75	3.75	0.8	8.0	120	On	JONSWAP waves, tide

at low tide (e.g. $h_S = 1.75$ m) followed by six segments for the rising tide (e.g. 1.75 m$<h_S<$3.00 m), and one segment at high tide (e.g. $h_S = 3.25$ m). In some cases, this was then followed by a further six segments for the falling tide (e.g. 3.00$<h_S>$1.75 m). The JONSWAP wave steering signal used for each tidal segment was identical and based on the average h_S value at any given tidal stage (e.g. Fig. 3b). This ensured that the morphological response of the barrier was not attributable to changing wave conditions. Continuity was obtained by tapering the design wave conditions to zero at the start and end of each stage and by concatenation of all the wave signals from each tidal stage. Although the use of an average h_S value for each tidal stage resulted in wave height statistics that differed slightly from the design specification due to the continuous change in water level, it is considered that this did not adversely affect the

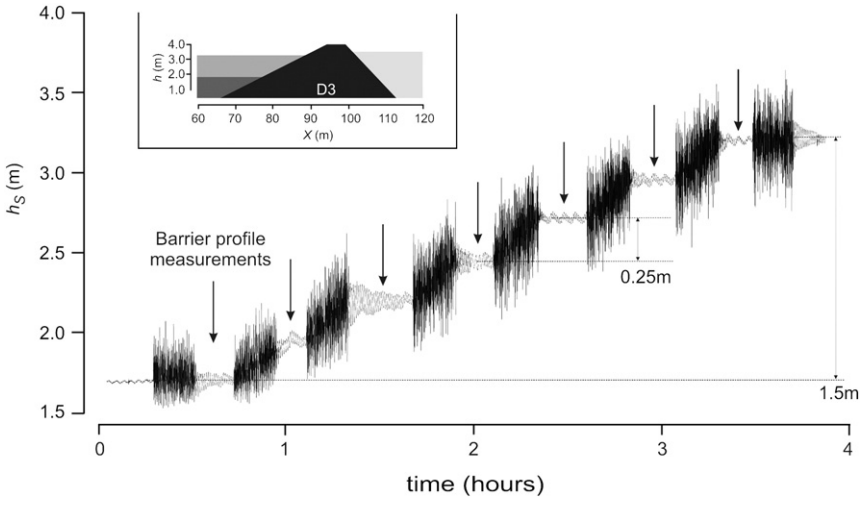

Fig. 7. Time-series showing rising mean water levels with superimposed waves during test *D3*.

Fig. 8. Typical barrier overwash sequence during simulations of storm conditions and high tidal levels.

experiments. The tidal sequence used in test *D2* in Fig. 7 shows rising mean water levels with superimposed waves and indicates the times when barrier profiles were measured. The inset in Fig. 7 shows an overview of water levels during the test.

With the exception of one 'reset' before test D1 (Table 2) *Test Series D* and *E* proceeded in an orderly sequence and involved raising or lowering h_S in steps to simulate a tide whilst at the same time maintaining a constant h_L value. Additionally, tests *E2* and *E5* maintained constant h_S and h_L values and examined barrier responses to changing wave conditions. These tests were designed to determine the thresholds required for incipient overwash. Other tests in *Series E* were undertaken to study the morphological response of the barrier under full overwash conditions. Particle tracing experiments outlined above were undertaken during this *Test Series*. An illustration of a barrier overwash sequence is shown in Fig. 8. Even in these high energy conditions, instruments on the barrier frame functioned well and data related to overwash flow speed and depths were obtained.

5. Summary

A number of aspects of the BARDEX project are novel: (1) gravel beach research in the laboratory is relatively rare, especially on this scale (the notable exception being the GWK experiments reported by Blanco (2002); (2) the experiments are believed to be the first combining waves with variations of offshore and lagoon water levels; and (3) the state-of-the-art measurements, including turbulence, run-up, sub-tidal, intertidal and supra-tidal bed morphologies, sediment size, and groundwater table are some of the most detailed ever undertaken in a laboratory study of a gravel beach. The experiments have, for the first time, examined the response of a gravel barrier beach to different water levels either side of the barrier in the presence of waves and to overwash events. The use of metered high capacity pumps has allowed water levels to be held at different relative levels either side of the barrier and have enabled direct measurements of hydraulic conductivity. It is considered that the data set collected will therefore be of interest to the wider academic community in the fields of coastal hydrodynamics and hydraulics, coastal defence and geotechnics, and nearshore morphodynamics and sediment transport. Further, the outcomes from the various detailed studies reported in this special issue will be of interest to engineers tasked with designing a range of gravel beach schemes and to coastal managers with responsibility for safety, conservation and preservation of existing gravel beaches.

Acknowledgements

The data reported here were collected in the Delta flume (Netherlands) as part of the EU-funded BARDEX project (HYDRALAB III Contract no. 022441 (RII3), Barrier Dynamics Experiments).

References

Austin, M.J., Buscombe, D., 2008. Morphological change and sediment dynamics of the beach step on a macrotidal gravel beach. Marine Geology 249, 167–183.
Austin, M.J., Masselink, G., 2006a. Swash-groundwater interaction on a steep gravel beach. Continental Shelf Research 26 (20), 2503–2519.
Austin, M.J., Masselink, G., 2006b. Observations of morphological change and sediment transport on a steep gravel beach. Marine Geology 229 (1–2), 59–77.
Battjes, J.A., Van Vledder, G.P., 1984. Verification of Kimura's theory for wave group statistics. Proceedings ICCE'84 43, 642–648.
Bishop, C.T., Donelan, M.A., 1987. Measuring waves with pressure transducers. Coastal Engineering 11, 309–328.
Blanco, B., 2002. Large wave channel (GWK) experiments on gravel and mixed beaches. Experimental Procedure and Data Documentation. Rept. TR-130, HR Wallingford.
Bradbury, A.P., 2000. Predicting breaching of shingle barrier beaches — recent advances to aid beach management. Proc. 35th MAFF (Defra) Conf. on River and Coastal Eng, pp. 05.3.1–05.3.13.
Bradbury, A.P., McCabe, M., 2003. Morphodynamic response of shingle and mixed sand/shingle beaches in large scale tests—preliminary observations. Proc. Hydralab II, Budapest, pp. 9-1–9-11.
Bradbury, A., Powell, K., 1992. The short term profile response of shingle spits to storm wave action. Proceedings of the International Conference Coastal Engineering, ASCE 2694–2707.
Buscombe, D., 2008. Estimation of grain size distributions and associated parameters from digital images of sediment. Sedimentary Geology 210, 1–10.
Buscombe, D., Masselink, G., 2009. Grain size information from the statistical properties of digital images of sediment. Sedimentology 56, 421–438.
Buscombe, D., Williams, J.J., Masselink, G., 2008. BARDEX: Experimental procedures, technical information and data report. School of Geography, Univ. Plymouth, UK, 164pp. unpublished manuscript.Now available from University of Plymouth, subject to a handling fee.
Butt, T., Russell, P., Turner, I., 2001. The influence of swash infiltration-exfiltration on beach face sediment transport: onshore or offshore? Coastal Engineering 42 (1), 35–52.
Chadwick, A.J., Karunarathna, H., Gehrels, W.R., O'Brien, D., Dales, D., 2005. A new analysis of the Slapton Barrier beach system. UK. Proceedings of the Institution of Civil Engineers: Maritime Engineering 158 (4), 147–161.
Folk, R.L., Ward, W.C., 1957. Brazos river bar: a study of significance of grain size parameters. Journal of Sedimentary Petrology 27, 3–26.
Forbes, D.L., Taylor, R.B., Orford, J.D., Carter, R.W.G., Shaw, J., 1991. Gravel-barrier migration and overstepping. Marine Geology 97 (3–4), 305–313.
Horn, D.P., 2006. Measurements and modelling of beach ground-water flow in the swash-zone: a review. Continental Shelf Research 26, 622–652.
Kroon, A., Larson, M., Möller, I., Yokoki, H., Rozynski, G., Cox, J., Larroude, P., 2008. Statistical analysis of coastal morphological data sets over seasonal to decadal time scales. Coastal Engineering 55 (7–8), 581–600.
Lawrence, J., Karunarathna, H., Chadwick, A.J., Flemming, C., 2002. Cross-shore sediment transport on mixed coarse grain sized beaches: modelling and measurements. Proc. 28th Int. Conf. Coastal Eng., ASCE, pp. 2565–2577.
Long, A.J., Waller, M.P., Plater, A.J., 2006. Coastal resilience and late Holocene tidal inlet history: the evolution of Dungeness foreland and the Romney Marsh depositional complex (UK). Geomorphologie 82 (3–4), 309–330.
Mansard, E.P.D., Funk, E.R., 1980. The measurement of incident and reflected spectra using a least squares method. Proc. Coastal Eng., ASCE, pp. 154–172.
Mason, T., Coates, T.T., 2001. Sediment transport processes on mixed beaches: a review for shoreline management. Journal of Coastal Research 17 (3), 645–657.
Masselink, G., Buscombe, D., 2008. Shifting gravel: a case study of Slapton Sands. Geographical Review 22 (1), 27–31.
Masselink, G., Short, A., 1993. The influence of tide range on beach morphodynamics: a conceptual model. Journal of Coastal Research 9, 785–800.
Masselink, G., Austin, M., Tinker, J., O'Hare, T., Russell, P.E., 2009. Cross-shore sediment transport and morphological response on a macro-tidal beach with intertidal bar morphology, Truc Vert, France. Marine Geology 251, 141–155. doi:10.1016/j.margeo.2008.01.010.
Moses, C.A., Williams, R.B.G., 2008. Artificial beach recharge: the South East England experience. Zeitschrift fur Geomorphologie N.E. 52 (3), 107–124.

Obhrai, C., Powell, K., Bradbury, A., 2008. A laboratory study of overtopping and breaching of shingle barrier beaches. Proc. Coastal Engineering, Hannover, Germany, pp. 1497–1508.
Orford, J.D., Carter, R.W.G., Forbes, D.L., Taylor, R.B., 1988. Overwash occurrence consequent on morphodynamic changes following lagoon outlet closure on a coarse clastic barrier. Earth Surface Processes and Landforms 13 (1), 27–35.
Orford, J.D., Carter, R., Jennings, S., 1996. Control domains and morphological phases in gravel-dominated coastal barriers of Nova Scotia. Journal of Coastal Research 12 (3), 589–604.
Orford, J.D., Forbes, D.L., Jennings, S.C., 2002. Organisational controls, typologies and time scales of paraglacial gravel-dominated coastal systems. Geomorphology 48 (1–3), 51–85.
Orford, J.D., Jennings, S., Pethick, J., 2003. Extreme storm effect on gravel dominated barriers. Proceedings of the International Conference on Coastal Sediments 2003. CD-ROM published by World Scientific Publishing Corp. and East Meets West Productions, Corpus Christi, Texas, USA. ISBN 981-238-422-7, 12pp.
Pedrozo-Acuna, A., Simmonds, D.J., Otta, A.K., Chadwick, A.J., 2006. On the cross-shore profile change of gravel beaches. Coastal Engineering 53 (4), 335–347.
Pedrozo-Acuna, A., Simmonds, D.J., Chadwick, A.J., Silva, R., 2007. A numerical-empirical approach for evaluating morphodynamic processes on gravel and mixed sand-gravel beaches. Marine Geology 241 (1–4), 1–18.
Plater, A.J., Stupples, P., Roberts, H.M., 2009. Evidence of episodic coastal change during the late Holocene: the Dungeness barrier complex, SE England. Geomorphologie 104 (1–2), 47–58.
Puleo, J.A., 2009. Tidal variability of swash-zone sediment suspension and transport. Journal of Coastal Research 25 (4), 937–948. doi:10.2112/08-1031.1.
Pye, K., Blott, S.J., 2009. Progressive breakdown of a gravel-dominated coastal barrier, Dunwich-Walberswick, Suffolk, UK: processes and implications. Journal of Coastal Research 25 (3), 589–602.
Riddell, K.J., Young, S.W., 1992. The management and creation of beaches for coastal defence. Water Environment Journal 6 (6), 588–597.
Roelvink, J.A., Reniers, A.J.H.M., 1995. LIP11 D Deltaflume experiment: dataset for profile validation. Rept. H2130 Delft Hydraulics, Delft, Netherlands.
Rubin, D.M., 2004. A simple autocorrelation algorithm for determining grain size from digital images of sediment. Journal of Sedimentary Research 74, 160–165.
Shulmeister, J., Kirk, R.M., 1997. Holocene fluvial-coastal interactions on a mixed sand and sand and gravel beach system, North Canterbury, New Zealand. Catena 30 (4), 337–355.
Trim, L.K., She, K., Pope, D.J., 2002. Tidal effects on cross-shore sediment transport on a shingle beach. Journal of Coastal Research SI36, 708–715.
Turner, I.L., Masselink, G., 1998. Swash infiltration-exfiltration and sediment transport. Journal of Geophysical Research 103/C13, 30813–30824.
Turner, I.L., Russell, P.E., Butt, T., 2008. Measurement of wave-by-wave bed-levels in the swash zone. Coastal Engineering. doi:10.1016/j.coastaleng.2008.09.009.
Van Wellen, E., Chadwick, A.J., Mason, T., 2000. A review and assessment of longshore sediment transport equations for coarse grained beaches. Coastal Engineering 40 (3), 243–275.